*Chinese Journal of*
**POLYMER SCIENCE**

RESEARCH ARTICLE

https://doi.org/10.1007/s10118-024-3109-5
*Chinese J. Polym. Sci.*

# Bioinspired Double-stranded Yarn with Alternating Hydrophobic/Hydrophilic Patterns for High-efficiency Fog Collection

Lan-Lan Hou[a,c], Meng-Na Qiu[b], Ya-Qiong Wang[b], Tong-Hua Bai[b], Zhi-Min Cui[b], Jing-Chong Liu[d], Ying-Qun Qi[a], Nü Wang[b], Yong Li[c*], and Yong Zhao[b*]

[a] *Beijing Institute of Graphic Communication, Beijing 102600, China*
[b] *Key Laboratory of Bioinspired Smart Interfacial Science and Technology of Ministry of Education, Beijing Key Laboratory of Bioinspired Energy Materials and Devices, School of Chemistry, Beijing Advanced Innovation Center for Biomedical Engineering, Beihang University, Beijing 100191, China*
[c] *Key Laboratory of Cryogenics, Technical Institute of Physics and Chemistry, Chinese Academy of Sciences, Beijing 100190, China*
[d] *Beijing Key Laboratory for Bioengineering and Sensing, Technology, Daxing Research Institute, School of Chemistry and Biological Engineering, University of Science and Technology Beijing, Beijing 100083, China*

Electronic Supplementary Information

**Abstract** Efforts to develop innovative water harvesting strategies offer powerful solutions to alleviate the water crisis, especially in remote and arid areas. Inspired by the hydrophobic/hydrophilic pattern of desert beetles and water self-propulsion property of spider silks, a double-strand hydrophobic PVDF-HFP/hydrophilic PAN nanofibers yarn is proposed by electrospinning and twisting techniques. The double-strand cooperation approach allows for water deposition on hydrophobic PVDF-HFP segment and transport under the asymmetric capillary driving force of hydrophilic PAN segment, thus speeded up the aggregation and growth of droplets. The effects of the composition and the diameter ratio of the two primary yarns were studied and optimized for boosting fog collection performance. The double-strand anisotropic yarn not only provide an effective method for water harvesting, but also hold the potential to inspire innovative design concepts for fog collection materials in challenging environments.

**Keywords** Fog collection; Wettability; Electrospinning; Nanofibers; Spider silk

**Citation:** Hou, L. L.; Qiu, M. N.; Wang, Y. Q.; Bai, T. H.; Cui, Z. M.; Liu, J. C.; Qi, Y. Q.; Wang, N.; Li, Y.; Zhao, Y. Bioinspired double-stranded yarn with alternating hydrophobic/hydrophilic patterns for high-efficiency fog collection. *Chinese J. Polym. Sci.* https://doi.org/10.1007/s10118-024-3109-5

## INTRODUCTION

Nowadays, shortage of water resource is becoming an increasingly serious global problem.[1–3] Despite surface fresh water has been fully or even over-exploited, it is often overlooked that the air holds a significant amount of water. Accordingly, there is increasing interest in producing fresh water from atmosphere.[4,5] Fog harvesting offers a potential strategy for accessing of drinking water resources. In order to collect these "invisible" water, various methods have been explored, such as vapor compression, Peltier cooling, as well as absorption-based hygroscopic salts, porous gels, and MOFs.[6–11] However, the critical problems are the time-consuming and high energy consumption in the process of water release and systems regeneration. Nature provides researchers with more flexible and effective inspirations.[12–17] Numerous organisms in the natural world possess remarkable abilities for water collection, such as desert beetles, spider silk, *Nepenthes*,[18] *Sarraceia*, cactus[19] and water transportation like shorebird,[20] butterfly,[21] owing to their precisely designed surface texture arrangements at the micro/nanoscale. Of particular interest are the hydrophobic/hydrophilic patterned backs of desert beetles[22] along with the periodic spindle-knots and joint structures in spider silk,[23] which have garnered a great deal of attention. The back of Namib beetle consists of alternating wax-coated hydrophobic and non-waxy hydrophilic microdomains, morning fog can be captured on the discrete hydrophilic sites and grow up to water droplets, then droplets are directed towards the mouth of beetle along the hydrophobic areas that is conductive to transport the water droplets. In addition, spider silks can collect and transport water by virtue of their periodic spindle-knots and joints based on geometry induced Laplace pressure difference.[23] In recent years, based on diverse well-designed micro-multilevel structures and surface compositions, researchers have made remarkable advances in fog harvesting through the application of bionic systems.[24–30] High-efficient fog collection is closely related to two main factors that include rapid droplet capture and directional water transport.[31,32] The crucial to high performances are the

* Corresponding authors, E-mail: liyong1897@mail.ipc.ac.cn (Y.L.)
E-mail: zhaoyong@buaa.edu.cn (Y.Z.)

Special Issue: Functional Polymer Materials
Received January 28, 2024; Accepted February 21, 2024; Published online April 10, 2024

precise control and coordination of the microstructure design for geometry, shape, scale, and surface wetting modulation of solid surface in droplets behavior manipulation. For example, surface with star-shaped wettability patterns,[33] and of hierarchical wedge-shaped tracks,[34] and superhydrophilic arrays with wedge structure and slippery feature,[35] as well as various integrated anisotropic Janus systems[36–39] are dedicated to improve fog collection efficiency by regulating water condensation, coalescence and transportation. Artificial spider silks of diverse chemical compositions and surface structures also have made substantial advances, enabling droplets to coalesce and be transported directionally toward humps for fog harvesting.[40–44] Moreover, these have further been woven into webs that can be used for large-area water collection operations.[45–47]

Both desert beetles and spider silks have evolved remarkable water-harvesting capabilities, the evolutionary purpose of these are to meet their specific water requirements to thrive in arid environments. Nonetheless, the total water-collecting capacity of these insects is still limited because the body figure of these insects is quite small. As a result, directly applying and scaling these biological water-harvesting concepts present challenges in meeting the genuine needs of humanity. For instance, the artificial model of the beetle's back features a two-dimensional (2D) solid plane surface that impedes the passage of wind. While this design is suitable for smaller area water collection, scaling it up becomes problematic due to wind obstruction. This scaling issue also results in increased material costs and decreased water collection efficiency. On the other hand, one-dimensional (1D) artificial spider silk material does not obstruct wind flow and can be produced more affordably for larger areas. However, the key for efficient water collection lies in its periodic protruding knot structure, which has a very thin optimal diameter (often micron to tens of micron) comparable to that of fog droplets. This implies that the mechanical strength of artificial spider silk fibers is relatively low, often resulting in failure to withstand natural wind conditions. While increasing the fiber diameter can enhance strength, it comes at the cost of sacrificing water collection efficiency. Thus, developing a spider silk-inspired water harvesting system that does not hinder wind movement and balances both robust mechanical strength and water collection efficiency remains a significant challenge.

Herein, seeking wisdom from nature, we presented a double-strand nanofibers yarn with stripe-patterned opposite wettability that drawn complementary advantages inspiration from desert beetles and spider silk, which exhibits highly efficient fog harvesting properties as well as high mechanical strength. The double-strand yarn, featuring anisotropic wettability, are meticulously constructed by double-twisting of the primary hydrophilic nanofibers yarn and hydrophobic nanofibers yarn. The water collection rate of anisotropic yarn reached 3.20±0.13 $g \cdot h^{-1} \cdot cm^{-2}$ that outperformed homogeneous hydrophilic or hydrophobic counterpart yarns. The high fog collection performance is benefit from the synergistic effect of water trapping at the hydrophobic sites, along with self-transporting of water droplets towards the hydrophilic region, which facilitate the convergence and collection of water. This concept of double-strand cooperative anisotropic yarn is expected to inspire new ideas for the design and applications of high-performance water collection materials.

## EXPERIMENTAL

### Materials

*N*,*N*-dimethylformamide (DMF), *N*,*N*-dimethylacetamide (DMAc) and acetone were purchased from Beijing Chemical Works. Poly(vinylidene fluoride-*co*-hexafluoropropylene) (PVDF-HFP) and polyacrylonitrile (PAN) were purchased from Sigma-Aldrich, Shanghai, China and used as received.

### Preparation of Fibrous Membranes with Opposite Wettability

The PVDF-HFP (15 wt%) was dissolved in a mixture of acetone and DMAc (7/3, *W*/*W*) The PAN (10 wt%) was dissolved in DMF. The PVDF-HFP and PAN precursors were electrospun to nanofibrous films under working voltage and receiving distance of 14 kV, 15 cm and 16 kV, 15 cm, respectively.

### Preparation of Double-strand Anisotropic Twisted Yarn

The as-prepared electrospinning membranes were cut in rectangle strip with dimensions of 2 cm × 15 cm and then mounted on electric motor to twist primary PAN and PVDF-HFP yarns, respectively. Then a PAN yarn and a PVDF-HFP yarn were secondary co-twisted to a double-strand yarn.

### Fog Collection Measurements

A stimulated fog flow was produced by a commercial humidifier. The as-prepared yarns were immobilized under the fog flow with an effective length of 4 cm at approximately 25 °C. The distance between as-prepared yarns and fog outlet was about 10 cm. The collected water dripped down from the as-prepared yarns by gravity and was gathered by a water container under the yarns. To calculate the water collection efficiency per unit area, the yarn area is calculated by considering the fiber cross-section as a regular circle. The calculation involves multiplying the perimeter of the cross-section by the length of the yarn.

### Characterizations

The scanning electron microscopy (SEM) images were obtained using a field emission scanning electron microscope (JEOL, JSM-7500F). The element energy dispersive spectroscopy (EDS) mapping images were collected by a JEOL JEM-ARM200F equipment. The contact angles were measured by an OCA20 instrument (Data-Physics, Germany) at ambient temperature. The performances of fog collection were recorded by a high-speed camera (Basler, acA1600-60gm). Mechanical properties of the yarns were assessed using the stress-strain test by an electrical universal material machine (SHIMADZU, AGS-X 1KN, Japan).

## RESULTS AND DISCUSSION

Two representative water harvesting biological samples in nature, *i.e.* Namib desert beetles and spider silk, are exemplified in Figs. 1(a) and 1(b). Fig. 1(a) shows a Namib desert beetle and its peak-valley structured back with bumped non-waxy hydrophilic regions and wax-coated hydrophobic valley regions that could be abstracted as a 2D surface with alternating hy-

https://doi.org/10.1007/s10118-024-3109-5

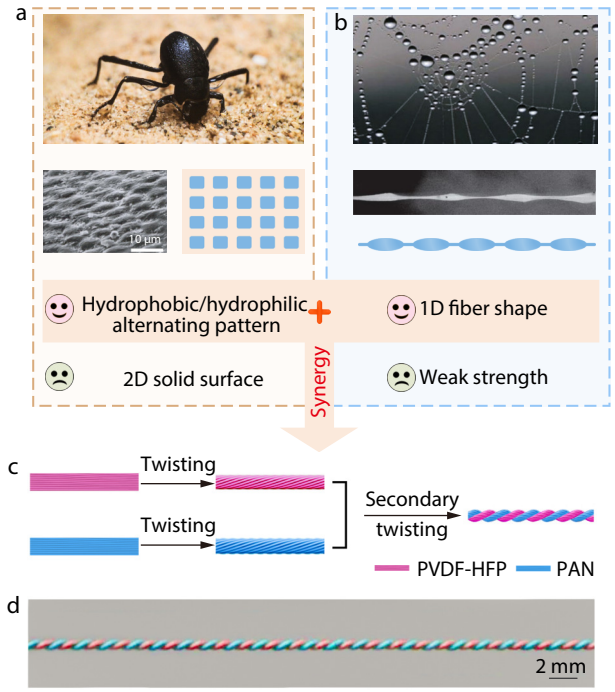


**Fig. 1** Schematic illustration of the biological fog collection models and preparation process of the double-strand anisotropic twisted yarn. (a) Namib desert beetle[48] and (b) spider silk[15] in nature with fog collection ability. The back of desert beetle is 2D with surface alternating hydrophobic/hydrophilic mosaic domains.[22] Spider silk is 1D structure with periodic spindle knot-slim joint structures.[23] The drawbacks of artificial large-scale fabrication of these two materials are that 2D structure is wind block and material consuming, while slim joints on 1D structure are weak spots of mechanical strength. (c) The preparation procedure of the hydrophobic PVDF-HFP/hydrophilic PAN double-strand anisotropic twisted yarn, which consists of three-steps including electrospinning, twisting, and secondary twisting. The double-strand yarn has 1D structure with alternating wettability that combines the advantages of desert beetle and spider silk while conquers their drawbacks. (d) Optical photograph of the PVDF-HFP (red)/PAN (blue) double-strand yarn.

drophobic/hydrophilic domains. Fig. 1(b) is the structure of spider silk with periodic spindle-knots and joints that can be regarded as a 1D object with periodic geometry gradient. Although these two kinds of natural fog collection architectures are very successful for the survive of the tiny body figure beetles and spiders in arid environment. However, large scale fabrication and applications of these nature-inspired artificial fog collection materials has encountered great obstacles. For examples, large area 2D structure is wind-block and huge material consumption, say nothing of the potential safety hazard in strong wind, while the 1D spider-silk-like periodic spindle structure has numerous slim joints that are bottlenecks for enough mechanical strength in real applications. These natural exemplary creatures have prompted us to integrate the advantages of the Namib desert beetles, characterized by its patterned wettability surface, and spider silk, known for its water self-propelled capabilities for 1D fibrous material.

As a result, we designed a bionic secondary-twisted anisotropic double-strand nanofibers yarn with opposite wettability for fog collection as illustrated in Fig. 1(c), which conquers the drawbacks of wind-block 2D materials and weak strength 1D materials. Initially, two membranes comprising aligned nanofibers of hydrophobic poly(vinylidene fluoride-*co*-hexafluoropropylene) (PVDF-HFP) and hydrophilic polyacrylonitrile (PAN) were obtained on a roller receiver through electrospinning. Subsequently, the aligned PVDF-HFP and PAN nanofibers were individually twisted to produce primary PVDF-HFP and primary PAN yarns. Then the primary PVDF-HFP yarn and PAN yarn were secondary-twisted to double-strand anisotropic yarn (Fig. S1 in the electronic supplementary information, ESI). The photograph in Fig. 1(d) depicts the double-strand anisotropic twisted yarn, with red PVDF-HFP (colored by Sudan II) alternating with blue PAN (colored by methylene blue).

The scanning electron microscopy (SEM) images in Figs. 2(a) and 2(b) display the uniform and aligned structure of the electrospun PVDF-HFP and PAN fibers, with average diameters of approximately 422±45 and 449±43 nm, respectively. The primary twisted PVDF-HFP (left) and PAN (right) yarns have a diameter of ~300 μm. These yarns exhibit numerous interconnected channels and a multilevel structure due to their helically aligned nanofibers organizations. Fig. 2(c) depicts the mechanical properties of three kind of double-strand yarns. Additionally, these structures and features will contribute to water collection and self-propulsion capabilities in application scenarios.[30,49,50] Two strand of PVDF-HFP and PAN yarns were combined and secondary twisted to double-strand homogeneous PVDF-HFP/PVDF-HFP, PAN/PAN yarns and heterogeneous PVDF-HFP/PAN yarn, respectively (Figs. 2d–2f). The different chemical composition of the three kinds of yarns was characterized by EDS elemental maps of representative elements fluorine (F, colored with green) in PVDF-HFP and nitrogen (N, colored with red) in PAN as shown in Figs. 2(g)–2(i). Unlike the homogeneous composition in Figs. 2(g) and 2(h), it is seen both N and F elements could be observed in PVDF-HFP/PAN yarn (Fig. 2i), which confirm the successfully integrating of the heterogeneous components. The wettability of the different yarns was then tested (see Figs. S2 and S3 in ESI for the wettability of the fiber membrane and primary yarn). It is seen the PVDF-HFP/PVDF-HFP yarn showed a water contact angle of 133.6°±2.1° indicating its highly hydrophobic property (Fig. 2j), while the PAN/PAN yarn displayed highly hydrophilic property that water could be completely absorbed into the yarn (Fig. 2k). Differently, PVDF-HFP/PAN double-strand yarn demonstrated anisotropic wettability with alternating hydrophobic and hydrophilic patterns in Fig. 2(l), that provide their desert-beetle-like property for fog collection.[22]

Fig. 3 illustrates the fog collection capabilities of the three types of double-strand yarns. We used a homemade fog-harvesting apparatus to quantitatively characterize the fog collection efficiency (Fig. 3a). In this work, we selected a double-strand PVDF-HFP/PAN yarn with a diameter of ~450 μm, an optimized diameter that shows excellent performance (Figs. S4 and S5 in ESI). In Fig. 3(b), the fog collection efficiencies of PAN/PAN and PVDF-HFP/PVDF-HFP double-strand yarns were 0.90±0.11 and 2.55±0.16 $g \cdot h^{-1} \cdot cm^{-2}$, respectively. While the PVDF-HFP/PAN group with hybrid hydrophobicity-hy-

https://doi.org/10.1007/s10118-024-3109-5

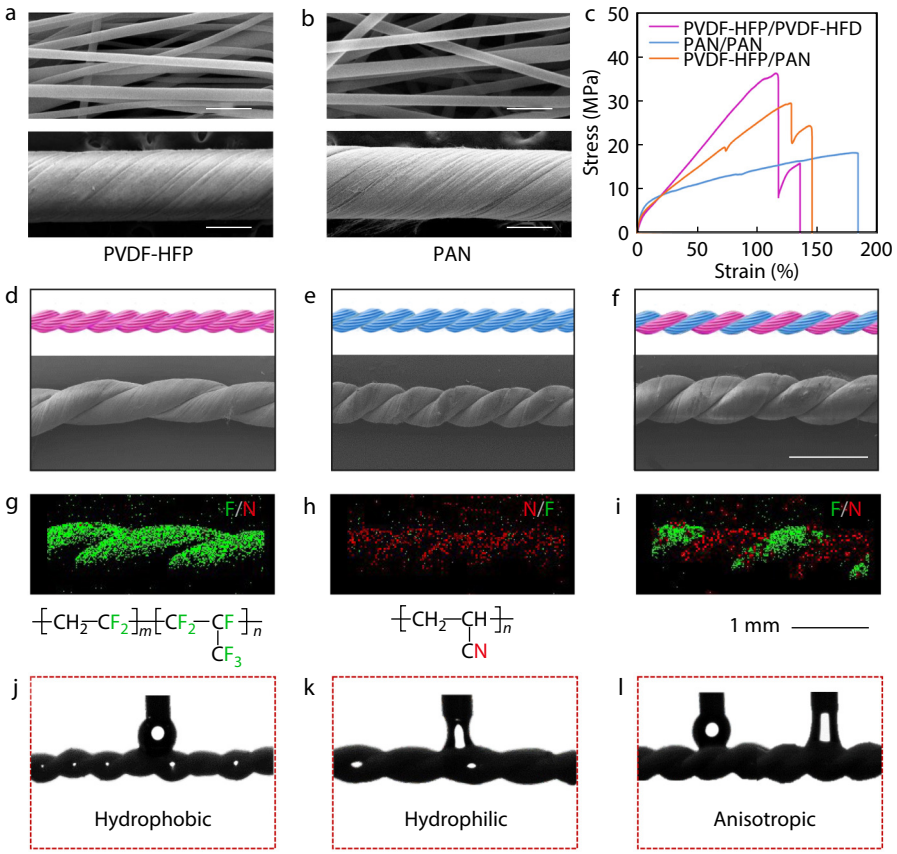


**Fig. 2** Morphology and wetting property. (a, b) SEM images of aligned PVDF-HFP and PAN fibers. The scale bar is 2 μm. As well as the primary twisted PVDF-HFP yarn and PAN yarn. The scale bar is 200 μm. (c) Mechanical property of three kind of double-strand yarns. (d–l) The three kinds of double-strand yarns of PVDF-HFP/PVDF-HFP, PAN/PAN and PVDF-HFP/PAN components: (d–f) Schematic illustrations and SEM images, (g–i) EDS maps of F and N elements indicate the heterogeneous composition of PVDF-HFP/PAN double-strand yarn, (j–l) the hydrophobic PVDF-HFP/PVDF-HFP yarn, the hydrophilic PAN/PAN yarn, and the PVDF-HFP/PAN double-stranded yarn shows alternating hydrophobicity/hydrophilicity.

drophilicity exhibited the highest water collection efficiency of 3.20±0.13 $g \cdot h^{-1} \cdot cm^{-2}$. It indicates the existence of the hydrophilic and hydrophobic patterned structures in the double-strand anisotropic twisted yarns promoted the aggregation of the droplets and thus greatly enhanced the speed of fog collection

Then the *in situ* real time fog collection process was observed as shown in Fig. 3(c). It is seen that the hydrophilic PAN/PAN yarn in fog tends to wet the whole yarns, forming a thin water film. However, this thin water film completely spread along the yarn due to the homogeneous hydrophilicity that does not accumulate into water droplets and cannot be collected for practical use.[51] In contrast, fog on the hydrophobic PVDF-HFP/PVDF-HFP yarn assembles into a lot of tiny droplets that *in situ* grew up along with time (Fig. 3d). However, this *in situ* growing mode is of low efficiency because the fog collection process accompanies with water evaporation at the same time. Therefore, the keypoint of a fog collecting material lies in how to accumulate larger water drops as soon as possible. In this regard, the double-strand PVDF-HFP/PAN yarn with anisotropic wettability exhibited much higher fog collection performance than above two samples (Fig. 3e). When the PVDF-HFP/PAN yarn is in a foggy environment, the hydrophobic PVDF-HFP domains mainly serve as the collection sites, while the hydrophilic PAN sites attract the water droplets beside the PVDF-HFP domains and facilitates the aggregation of these droplets onto larger water drops. The as-formed large water drops will fall into the underlying water container, transforming into usable fresh water. Consequently, the synergistic effect of the hydrophobic and hydrophilic patterns in the anisotropic PVDF-HFP/PAN yarn enhances the fog collection performances.

Fig. 4 illustrates the water collection mechanism of three types of double-strand anisotropic yarns. On PAN/PAN yarn as shown in Fig. 4(a), fog droplets are absorbed by the yarn due to the hydrophilicity, but they tend to form a thin water film rather than accumulating to larger water drops and being collected. On PVDF-HFP/PVDF-HFP (Fig. 4b), the hydrophobic yarn facilitates the deposition of numerous tiny droplets, but these droplets only *in situ* growth that is time-consuming and inefficient due to the accumulation/evaporation balance. Fig. 4(c) presents a cooperative mode on double-strand wettability anisotropic PVDF-HFP/PAN yarn. The water droplets are captured on hydrophobic regions, then they are transported to the nearby hydrophilic regions under the hydrophilic capillary forces. These droplets undergo deposition, transport, coalescence, and collection cycles on the yarn as further shown in Fig. 4(d). Initially, water droplets are

https://doi.org/10.1007/s10118-024-3109-5

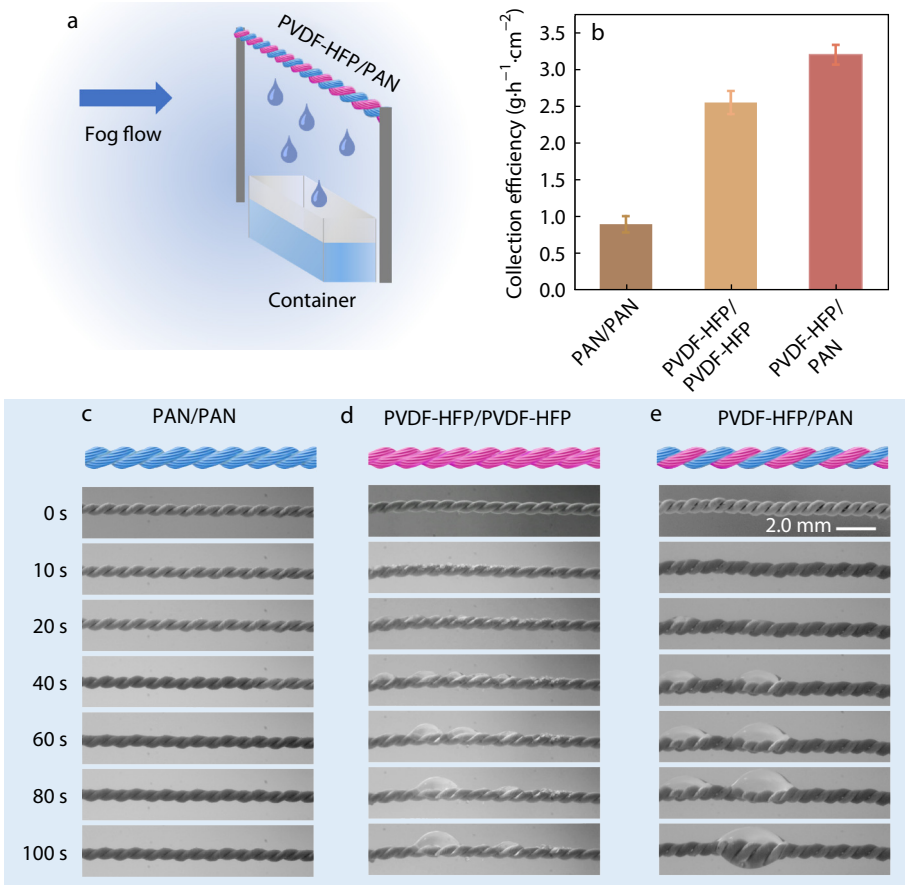


**Fig. 3** Fog collection performances on double-strand yarns with different components. (a) Schematic illustration of the fog collecting system; (b) Fog collection efficiency of PAN/PAN, PVDF-HFP/PVDF-HFP and PVDF-HFP/PAN yarns double-strand yarns that the PVDF-HFP/PAN yarn shows the highest efficiency; Process of fog collection on (c) PAN/PAN, (d) PVDF-HFP/PVDF-HFP and (e) PVDF-HFP/PAN yarns. It is seen the PVDF-HFP/PAN yarn accumulates the largest water droplet in same time.

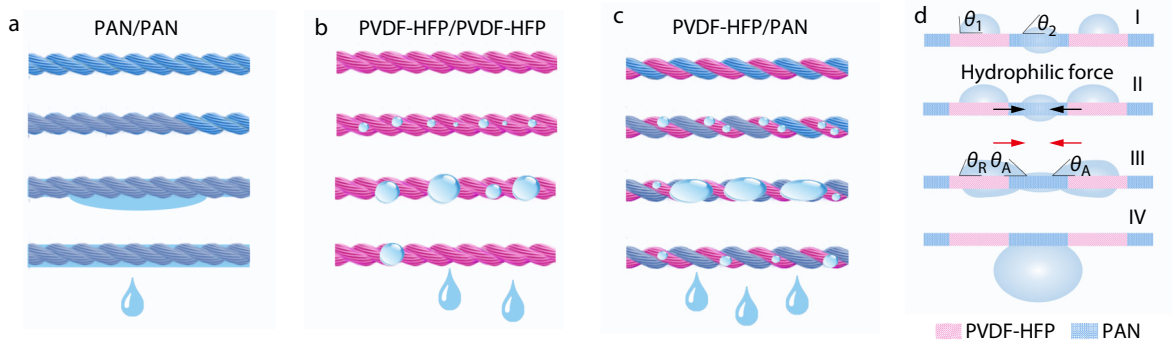


**Fig. 4** Fog collection mechanism on double-strand yarns. (a) Fog absorbed by hydrophilic PAN/PAN yarn and spread to a thin water film rather than collectable droplets; (b) Tiny droplets *in situ* steady growth on PVDF-HFP/PVDF-HFP yarn requires a considerable amount of time to form larger droplets; (c) Water droplets undergo a process of deposition, transport, coalescence, and be collected on anisotropic PVDF-HFP/PAN yarn; (d) The fog collection mechanism of PVDF-HFP/PAN yarn. Stage I: Fog droplets deposit and aggregate at the hydrophobic PVDF-HFP yarn sites. Stage II: Water droplets will be absorbed toward the hydrophilic PAN yarn region under the hydrophilic force. Stage III: The smaller water droplets spontaneously coalesce to larger drop due to gradient Laplace force that the advancing angle ($\theta_A$) in hydrophilic region is smaller than the receding angle ($\theta_R$) in hydrophobic region. Stage IV: Adjacent droplets rapidly merge to large water drop and then fall into water container achieving water collection target.

deposited and aggregated at the hydrophobic sites (stage I). Subsequently, the droplets self-propelled towards the hydrophilic regions under the wetting force (stage II). This driving force is generated from the gradient Laplace force[52–56]

$F = \int \gamma(\cos\theta_A - \cos\theta_R)\,dl$, where $\theta_A$ and $\theta_R$ are the advancing and receding contact angles of water drops on the hydrophilic region and hydrophobic region, respectively, $\gamma$ represents the surface tension of water, and $dl$ is the integral

https://doi.org/10.1007/s10118-024-3109-5

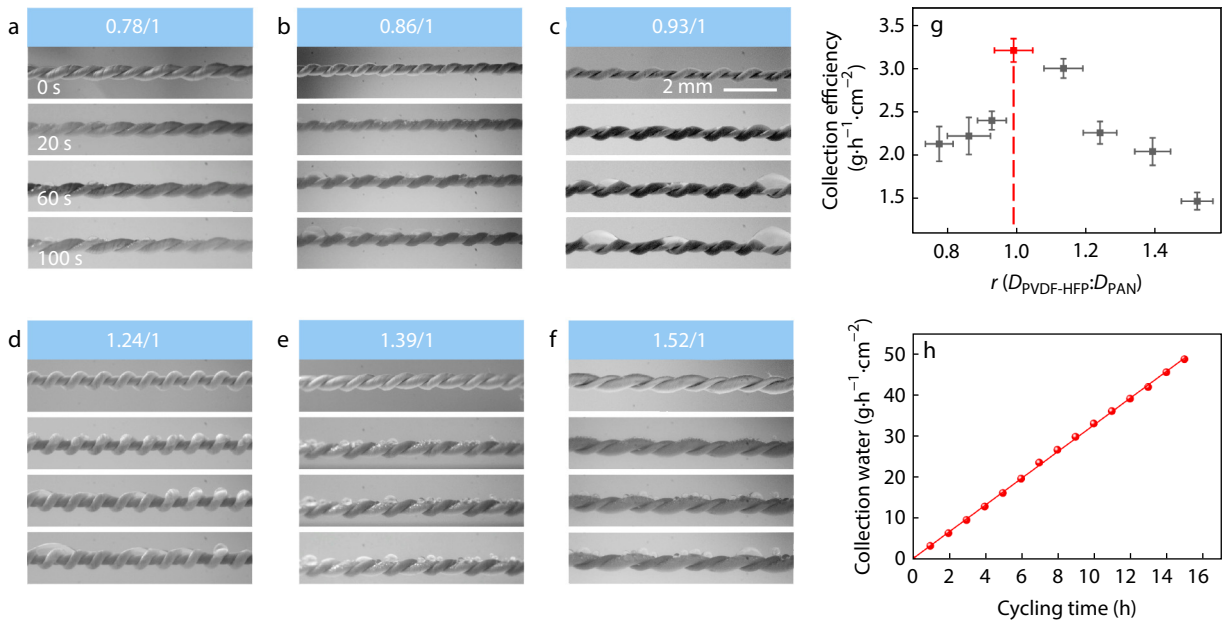


**Fig. 5** Influence of diameter ratio of PVDF-HFP to PAN on fog collection efficiency. (a–f) Fog collection process on double-strand yarns with different diameter ratio of PVDF-HFP to PAN primary yarn ($r = D_{PVDF\text{-}HFP}/D_{PAN}$ = 0.78, 0.86, 0.93, 1.24, 1.39 and 1.52, respectively); (g) Fog collection efficiency statistic of double-strand anisotropic twisted yarns with different diameter ratio showing the ratio 1:1 has the highest efficiency; (h) The stable water collection efficiency over 15 h.

variable along the length of the yarn. There is imbalance between the droplet advancing angle ($\theta_A$, smaller) and receding angle ($\theta_R$, larger) (stage III), causing the water droplets to move towards the hydrophilic regions. The adjacent droplets rapidly grow to large water drops and then fall in to the water container due to the gravity ultimately (stage IV). As a result, the double-strand PVDF-HFP/PAN yarn, featuring a stripe-patterned topographically opposite wettability, exhibits a significantly improved water collection efficiency in comparison to homogeneous PAN/PAN and PVDF-HFP/PVDF-HFP double-strand yarns.

In addition to the yarns' component, the fog collection efficiency of anisotropic yarn is also influenced by the diameter ratio of the primary single strand yarns. Consequently, double-strand yarns with varying diameter ratios ($r = D_{PVDF\text{-}HFP}/D_{PAN}$ = 0.78, 0.86, 0.93, 1.24, 1.39 and 1.52, respectively) were fabricated by adjusting the diameter of the primary yarns. Fig. 5(a) demonstrates that when the proportion of the hydrophobic PVDF-HFP region is insufficient for water deposition, the hydrophilic region takes precedence, water mainly spread along the yarn rather than accumulation to water drops on the yarn's surface. With PVDF-HFP/PAN increasing (as depicted in Figs. 5b and 5c), the hydrophobic deposition length expands that relatively larger water drops could be accumulated on the yarn. However, if the diameter ratio of PVDF-HFP/PAN yarn exceeds 1:1, as observed in Figs. 5(d)–5(f), the hydrophobic regions play a dominant role. Water droplets predominantly grow slowly *in situ* without aggregating, the coalescence of droplets becomes harder which also results in the decrease of water collection efficiency. Fig. 5(g) shows the statistical analysis of the water collection efficiency on double-strand yarn as a function of varying diameter ratio of PVDF-HFP yarn to PAN yarn (Fig. S6 in ESI). It is seen the efficiency exhibited a tendency of first rising and then falling, which reached apex of 3.20±0.13 g·h$^{-1}$·cm$^{-2}$ in 1:1. After parameter optimization, we conducted a long-term performance of water collection with a 1:1 PVDF-HFP/PAN yarn, as illustrated in Fig. 5(h) and Fig. S7 (in ESI). The results revealed its stable and high efficiency fog collection of cumulative 48.68 g·h$^{-1}$·cm$^{-2}$ over a 15-h duration.

## CONCLUSIONS

Drawing insights from the synergistic characteristics of Namib desert beetles and spider silk, we developed a hydrophobic/hydrophilic stripe-patterned double-strand yarn, which hold immense potential for highly efficient fog collection. The proportion of PVDF-HFP/PAN was strategically studied and optimized to achieve the best exposure of the hydrophobic segment, coupled with the asymmetric wetting driving force at the patterned junction, collectively facilitates rapid collection of water droplets. The PVDF-HFP/PAN double-strand yarn reaches its highest water collection rate of 3.20±0.13 g·h$^{-1}$·cm$^{-2}$. This very simple but effective synergistic strategy will inspire novel concepts for the next generation of fog-collecting materials, offering a promising solution for sustainable water resource management.

### Conflict of Interests

The authors declare no interest conflict.

### Electronic Supplementary Information

Electronic supplementary information (ESI) is available free of

https://doi.org/10.1007/s10118-024-3109-5

charge in the online version of this article at http://doi.org/10.1007/s10118-024-3109-5.

## Data Availability Statement

Data that should not be shared: The related data of this paper is data that should not be shared, and can be obtained from the author for reasonable reasons. The author's contact information: zhaoyong@buaa.edu.cn.

## ACKNOWLEDGMENTS

This work was financially supported by the National Natural Science Foundation of China (Nos. 22105012, 21975007, 22175007 and 52172080), Beijing Natural Science Foundation (Nos. 2242035, 2242041, 2232054 and 2232037), the National Natural Science Foundation for Outstanding Youth Foundation, the Fundamental Research Funds for the Central Universities, the National Program for Support of Top-notch Young Professionals, and the 111 project (No. B14009), the Youth Excellence Project of Beijing Institute of Graphic Communication (No. Ea202403) and the Scientific Research Foundation of Beijing Institute of Graphic Communication (No. 27170124031).

## REFERENCES

1 Gerbens-Leenes, W.; Hoekstra, A. Y. The water footprint of biofuel-based transport. *Energ. Environ. Sci.* **2011**, *4*, 2658–2668.
2 Shannon, M. A.; Bohn, P. W.; Elimelech, M.; Georgiadis, J. G.; Mariñas, B. J.; Mayes, A. M. Science and technology for water purification in the coming decades. *Nature* **2008**, *452*, 301–310.
3 Jeppesen, E.; Bekliolu, M.; Zkan, K.; Akyürek, Z. Salinization increase due to climate change will have substantial negative effects on inland waters: a call for multifaceted research at the local and global scale. *The Innovation* **2020**, *1*, 100030.
4 Gao, S.; Wang, Y.; Zhang, C.; Jiang, M.; Wang, S.; Wang, Z. Tailoring interfaces for atmospheric water harvesting: fundamentals and applications. *Matter* **2023**, *6*, 2182–2205.
5 Fathieh, F.; Kalmutzki, M. J.; Kapustin, E. A.; Waller, P. J.; Yang, J.; Yaghi, O. M. Practical water production from desert air. *Sci. Adv.* **2018**, *4*, eaat3198.
6 Salehi, A. A.; Ghannadi-Maragheh, M.; Torab-Mostaedi, M.; Torkaman, R.; Asadollahzadeh, M. A review on the water-energy nexus for drinking water production from humid air. *Renew. Sust. Energ. Rev.* **2020**, *120*, 109627.
7 Bilal, M.; Sultan, M.; Morosuk, T.; Den, W.; Sajjad, U.; Aslam, M. M. A.; Shahzad, M. W.; Farooq, M. Adsorption-based atmospheric water harvesting: a review of adsorbents and systems. *Int. Commun. Heat Mass* **2022**, *133*, 105961.
8 Eddaoudi, M.; Kim, J.; Rosi, N.; Vodak, D.; Wachter, J.; O'Keeffe, M.; Yaghi, O. M. Systematic design of pore size and functionality in isoreticular MOFs and their application in methane storage. *Science* **2002**, *295*, 469–472.
9 Graeber, G.; Diaz-Marin, C. D.; Gaugler, L. C.; Zhong, Y.; El Fil, B.; Liu, X.; Wang, E. N. Extreme water uptake of hygroscopic hydrogels through maximized swelling-induced salt loading. *Adv. Mater.* **2023**, *36*, 2211783.
10 Guo, Y.; Guan, W.; Lei, C.; Lu, H.; Shi, W.; Yu, G. Scalable super hygroscopic polymer films for sustainable moisture harvesting in arid environments. *Nat. Commun.* **2022**, *13*, 2761.
11 Song, Y.; Zeng, M.; Wang, X.; Shi, P.; Fei, M.; Zhu, J. Hierarchical engineering of sorption-based atmospheric water harvesters. *Adv. Mater.* **2023**, *36*, 2209134.
12 Hou, L.; Liu, X.; Ge, X.; Hu, R.; Cui, Z.; Wang, N.; Zhao, Y. Designing of anisotropic gradient surfaces for directional liquid transport: fundamentals, construction, and applications. *The Innovation* **2023**, *4*, 100508.
13 Hou, L.; Wang, N.; Wu, J.; Cui, Z.; Jiang, L.; Zhao, Y. Bioinspired superwettability electrospun micro/nanofibers and their applications. *Adv. Funct. Mater.* **2018**, *28*, 1801114.
14 Zhu, P.; Wang, L. Microfluidics-enabled soft manufacture of materials with tailorable wettability. *Chem. Rev.* **2022**, *122*, 7010–7060.
15 Ju, J.; Zheng, Y.; Jiang, L. Bioinspired one-dimensional materials for directional liquid transport. *Acc. Chem. Res.* **2014**, *47*, 2342–2352.
16 Tian, Y.; Su, B.; Jiang, L. Interfacial material system exhibiting superwettability. *Adv. Mater.* **2014**, *26*, 6872–6897.
17 Liu, K.; Cao, M.; Fujishima, A.; Jiang, L. Bio-inspired titanium dioxide materials with special wettability and their applications. *Chem. Rev.* **2014**, *114*, 10044–10094.
18 Chen, H.; Zhang, P.; Zhang, L.; Liu, H.; Jiang, Y.; Zhang, D.; Han, Z.; Jiang, L. Continuous directional water transport on the peristome surface of Nepenthes alata. *Nature* **2016**, *532*, 85–89.
19 Ju, J.; Bai, H.; Zheng, Y.; Zhao, T.; Fang, R.; Jiang, L. A multi-structural and multi-functional integrated fog collection system in cactus. *Nat. Commun.* **2012**, *3*, 1247.
20 Prakash, M.; Quéré, D.; Bush, J. W. M. Surface tension transport of prey by feeding shorebirds: the capillary ratchet. *Science* **2008**, *320*, 931–934.
21 Liu, C.; Ju, J.; Zheng, Y.; Jiang, L. Asymmetric ratchet effect for directional transport of fog drops on static and dynamic butterfly wings. *ACS Nano* **2014**, *8*, 1321–1329.
22 Parker, A. R.; Lawrence, C. R. Water capture by a desert beetle. *Nature* **2001**, *414*, 33–34.
23 Zheng, Y.; Bai, H.; Huang, Z.; Tian, X.; Nie, F. Q.; Zhao, Y.; Zhai, J.; Jiang, L. Directional water collection on wetted spider silk. *Nature* **2010**, *463*, 640–643.
24 Yu, Z.; Zhu, T.; Zhang, J.; Ge, M.; Fu, S.; Lai, Y. Fog harvesting devices inspired from single to multiple creatures: current progress and future perspective. *Adv. Funct. Mater.* **2022**, *32*, 2200359
25 Liu, X.; Li, B.; Gu, Z.; Zhou, K. 4D printing of butterfly scale-inspired structures for wide-angle directional liquid transport. *Small* **2023,** *19*, 2207640.
26 Li, C.; Liu, Y.; Gao, C.; Li, X.; Xing, Y.; Zheng, Y. Fog harvesting of a bioinspired nanocone-decorated 3D fiber network. *ACS Appl. Mater. Interfaces* **2019**, *11*, 4507–4513.
27 Liu, Y.; Yang, N.; Li, X.; Li, J.; Pei, W.; Xu, Y.; Hou, Y.; Zheng, Y. Water harvesting of bioinspired microfibers with rough spindle-knots from microfluidics. *Small* **2020**, *16*, 1901819.
28 Dai, X.; Sun, N.; Nielsen, S. O.; Stogin, B. B.; Wang, J.; Yang, S.; Wong, T. S. Hydrophilic directional slippery rough surfaces for water harvesting. *Sci. Adv.* **2018**, *4*, eaaq0919.
29 Tian, Y.; Zhu, P.; Tang, X.; Zhou, C.; Wang, J.; Kong, T.; Xu, M.; Wang, L. Large-scale water collection of bioinspired cavity-microfibers. *Nat. Commun.* **2017**, *8*, 1080.
30 Yu, Z.; Zhang, J.; Li, S.; Zhou, Z.; Qin, Z.; Liu, H.; Lai, Y.; Fu, S. Bio-inspired copper kirigami motifs leading to a 2D-3D switchable structure for programmable fog harvesting and water retention. *Adv. Funct. Mater.* **2023**, *33*, 2210730.
31 Ji, Y.; Yang, W.; Li, X.; Hou, K.; Du, P.; Zhao, H.; Fan, Z.; Xu, B.; Cai, Z. Thermodynamically induced interfacial condensation for efficient fog harvesting. *Small* **2023**, *19*, 2304037.
32 Luo, D.; Zhang, J.; Zeng, X.; Zhang, M.; Zeng, X.; Zhou, C.

Fabrication and target applications of hydrophilic-hydrophobic composite wettability surfaces based on surface wettability gradient and Laplace pressure gradient regulation. *Appl. Mater. Today* **2023**, *35*, 101957.
33 Bai, H.; Wang, L.; Ju, J.; Sun, R.; Zheng, Y.; Jiang, L. Efficient water collection on integrative bioinspired surfaces with star-shaped wettability patterns. *Adv. Mater.* **2014**, *26*, 5025−5030.
34 Lin, J.; Tan, X.; Shi, T.; Tang, Z.; Liao, G. Leaf vein-inspired hierarchical wedge-shaped tracks on flexible substrate for enhanced directional water collection. *ACS Appl. Mater. Interfaces* **2018**, *10*, 44815−44824.
35 Feng, R.; Song, F.; Xu, C.; Wang, X. L.; Wang, Y. Z. A quadruple-biomimetic surface for spontaneous and efficient fog harvesting. *Chem. Eng. J.* **2021**, *422*, 130119.
36 Cao, M.; Xiao, J.; Yu, C.; Li, K.; Jiang, L. Hydrophobic/hydrophilic cooperative Janus system for enhancement of fog collection. *Small* **2015**, *11*, 4379−4384.
37 Yin, K.; Du, H.; Dong, X.; Wang, C.; Duan, J. A.; He, J. A simple way to achieve bioinspired hybrid wettability surface with micro/nanopatterns for efficient fog collection. *Nanoscale* **2017**, *9*, 14620−14626.
38 Zhu, H.; Yang, F.; Li, J.; Guo, Z. High-efficiency water collection on biomimetic material with superwettable patterns. *Chem. Commun.* **2016**, *52*, 12415−12417.
39 Hu, R.; Wang, N.; Hou, L.; Cui, Z.; Liu, J.; Li, D.; Li, Q.; Zhang, H.; Zhao, Y. A bioinspired hybrid membrane with wettability and topology anisotropy for highly efficient fog collection. *J. Mater. Chem. A* **2019**, *7*, 124−132.
40 Tian, X.; Bai, H.; Zheng, Y.; Jiang, L. Bio-inspired heterostructured bead-on-string fibers that respond to environmental wetting. *Adv. Funct. Mater.* **2011**, *21*, 1398−1402.
41 Bai, H.; Tian, X.; Zheng, Y.; Ju, J.; Zhao, Y.; Jiang, L. Direction controlled driving of tiny water drops on bioinspired artificial spider silks. *Adv. Mater.* **2010**, *22*, 5521−5525.
42 Dong, H.; Wang, N.; Wang, L.; Bai, H.; Wu, J.; Zheng, Y.; Zhao, Y.; Jiang, L. Bioinspired electrospun knotted microfibers for fog harvesting. *Chemphyschem* **2012**, *13*, 1153−1156.
43 Chen, W.; Guo, Z. Hierarchical fibers for water collection inspired by spider silk. *Nanoscale* **2019**, *11*, 15448−15463.
44 Huan, J.; Chen, M.; Hou, Y.; Zheng, Y. Special fog harvesting mode on bioinspired hydrophilic dual-thread spider silk fiber. *Chem. Eng. J.* **2023**, *473*, 145174.
45 Liu, Y.; Yang, N.; Gao, C.; Li, X.; Guo, Z.; Hou, Y.; Zheng, Y. Bioinspired nanofibril-humped fibers with strong capillary channels for fog capture. *ACS Appl. Mater. Interfaces* **2020**, *12*, 28876−28884.
46 He, X. H.; Wang, W.; Liu, Y. M.; Jiang, M. Y.; Wu, F.; Deng, K.; Liu, Z.; Ju, X. J.; Xie, R.; Chu, L. Y. Microfluidic fabrication of bio-inspired microfibers with controllable magnetic spindle-knots for 3D assembly and water collection. *ACS Appl. Mater. Interfaces* **2015**, *7*, 17471−17481.
47 Venkatesan, H.; Chen, J.; Liu, H.; Liu, W.; Hu, J. A spider-capture-silk-like fiber with extremely high-volume directional water collection. *Adv. Funct. Mater.* **2020**, *30*, 2002437.
48 Chakrabarti, U.; Paoli, R.; Chatterjee, S.; Megaridis, C. M. Importance of body stance in fog droplet collection by the namib desert beetle. *Biomimetics* **2019**, *4*, 59.
49 Yi, S.; Wang, J.; Chen, Z.; Liu, B.; Ren, L.; Liang, L.; Jiang, L. Cactus-inspired conical spines with oriented microbarbs for efficient fog harvesting. *Adv. Mater. Technol.* **2019**, *4*, 1900727.
50 Liu, Z. A.; Liu, H.; Li, W.; Song, J. L. Optimization of bioinspired surfaces with enhanced water transportation capacity. *Chem. Eng. J.* **2022**, *433*, 134568.
51 Chen, H.; Ran, T.; Gan, Y.; Zhou, J.; Zhang, Y.; Zhang, L.; Zhang, D.; Jiang, L. Ultrafast water harvesting and transport in hierarchical microchannels. *Nat. Mater.* **2018**, *17*, 935−942.
52 Chaudhury, M. K.; Whitesides, G. M. How to make water run uphill. *Science* **1992**, *256*, 1539−1541.
53 Mazaltarim, A. J.; Bowen, J. J.; Taylor, J. M.; Morin, S. A. Dynamic manipulation of droplets using mechanically tunable microtextured chemical gradients. *Nat. Commun.* **2021**, *12*, 3114.
54 Daniel, S.; Chaudhury, M. K.; Chen, J. C. Fast drop movements resulting from the phase change on a gradient surface. *Science* **2001**, *291*, 633−636.
55 Thiele, U.; John, K.; Bär, M. Dynamical model for chemically driven running droplets. *Phys. Rev. Lett.* **2004**, *93*, 027802.
56 Hou, L.; Wang, N.; Yu, L. J.; Liu, J.; Zhang, S.; Cui, Z.; Li, S.; Li, H.; Liu, X.; Jiang, L.; Zhao, Y. High-performance Janus solar evaporator for water purification with broad spectrum absorption and ultralow heat loss. *ACS Energy Lett.* **2023**, *8*, 553−564.

https://doi.org/10.1007/s10118-024-3109-5